NeuroImage 227 (2021) 117643

Contents lists available at ScienceDirect

NeuroImage

journal homepage: www.elsevier.com/locate/neuroimage

White matter microstructure correlates of age, sex, handedness and motor ability in a population-based sample of 3031 school-age children

Mónica López-Vicente[a,b], Sander Lamballais[c,d], Suzanne Louwen[a], Manon Hillegers[a,b], Henning Tiemeier[a,d], Ryan L. Muetzel[a,*], Tonya White[a,e]

[a] Department of Child and Adolescent Psychiatry and Psychology, Erasmus MC University Medical Center, Rotterdam, the Netherlands
[b] The Generation R Study Group, Erasmus MC University Medical Center, Rotterdam, the Netherlands.
[c] Department of Epidemiology, Erasmus MC University Medical Center, Rotterdam, the Netherlands
[d] Department of Social and Behavioral Science, Harvard T. H. Chan School of Public Health, Boston, MA, USA
[e] Department of Radiology and Nuclear Medicine, Erasmus MC University Medical Center, Rotterdam, the Netherlands

ARTICLE INFO

Keywords:
Diffusion tensor imaging
General population
Finger tapping
Fractional anisotropy
White matter development

ABSTRACT

Understanding the development of white matter microstructure in the general population is an imperative precursor to identifying its involvement in psychopathology. Previous studies have reported changes in white matter microstructure associated with age and different developmental patterns between boys and girls. Handedness has also been related to white matter in adults. Motor performance, tightly dependent on overall neuronal myelination, has been related to the corpus callosum. However, the association between motor performance and global white matter microstructure has not been reported in the literature. In general, these age, sex, handedness, and motor performance associations have been observed using small and poorly representative samples. We examined the relationships between age, sex, handedness, and motor performance, measured with a finger tapping task, and white matter microstructure in the forceps major and minor and in 5 tracts bilaterally (cingulum, corticospinal, inferior and superior longitudinal fasciculi, and uncinate) in a population-based sample of 3031 children between 8 and 12 years of age. Diffusion tensor imaging (DTI) data were acquired using a single, study-dedicated 3 Tesla scanner. We extracted and quantified features of white matter microstructure for each tract. We computed global DTI metrics by combining scalar values across multiple tracts into single latent factors using a confirmatory factor analysis. The adjusted linear regression models indicated that age was associated with global fractional anisotropy (FA), global mean diffusivity (MD), and almost all the tracts. Further, girls showed lower global MD than boys, while FA values differed by tract, and no age-sex interactions were found. No differences were observed in white matter microstructure between right- and left-handed children. We observed that FA in forceps major was associated with right-hand finger tapping performance. White matter FA in association tracts was only related to motor function before multiple testing correction. Our findings do not provide evidence for a relationship between finger tapping task performance and global white matter microstructure.

1. Introduction

The development of white matter is a prolonged process that begins *in utero* and extends beyond early adulthood (Yakovlev and Lecours, 1967). White matter interconnects spatially segregated cortical and subcortical regions for fast and efficient information transfer and consists primarily of myelinated axons. The *in vivo* study of white matter microstructure in humans has been fostered by the introduction of diffusion tensor imaging (DTI) in mid 1990s (Basser et al., 1994). DTI is a magnetic resonance imaging (MRI) technique that probes white matter microstructure by measuring the magnitude and direction of water diffusion in the brain (Basser and Pierpaoli, 1996). Previous work has shown that white matter microstructure develops from infancy into adulthood (Giorgio et al., 2010, Lebel et al., 2008, Schmithorst and Yuan, 2010). As white matter disruptions are a common feature of several psychiatric disorders (Pasternak et al., 2018), understanding how white matter microstructure develops in the general population is an imperative precursor to identifying its involvement in psychopathology.

Abbreviations: AD, Axial diffusivity; CB, Cingulum bundle; CC, Corpus callosum; CST, Corticospinal tract; DTI, Diffusion tensor imaging; FA, Fractional anisotropy; FMa, Forceps major; FMi, Forceps minor; ILF, Inferior longitudinal fasciculus; IPW, Inverse probability weighting; MD, Mean diffusivity; MRI, Magnetic resonance imaging; SLF, Superior longitudinal fasciculus; RD, Radial diffusivity; UF, Uncinate fasciculus.

* Corresponding author.

https://doi.org/10.1016/j.neuroimage.2020.117643
Received 16 June 2020; Received in revised form 1 December 2020; Accepted 9 December 2020
Available online 15 December 2020

Numerous methods exist to extract and quantify features of white matter microstructure using DTI. For example, fiber tractography utilizes directional information embedded in diffusion weighted images to delineate sub-parcels of white matter anatomy. Fractional anisotropy (FA) and mean diffusivity (MD) are frequently used as measures of white matter microstructure. The values of parallel or axial diffusivity (AD) has been suggested to reflect axonal characteristics, while the perpendicular or radial diffusivity (RD) has been related to myelination (Eluvathingal et al., 2007). Cross-sectional (Lebel et al., 2008; Schmithorst and Yuan, 2010; Eluvathingal et al., 2007; Barnea-Goraly et al., 2005; Clayden et al., 2012; Lebel et al., 2010; Muftuler et al., 2012; Qiu et al., 2008) and longitudinal (Brouwer et al., 2012; Krogsrud et al., 2016; Simmonds et al., 2014) studies of brain development during childhood have largely demonstrated associations between age and these DTI-derived metrics, particularly with increases in FA and decreases in MD. Similar to studies of cortical morphology (Gogtay et al., 2004; Giedd et al., 1999), some spatial patterns in timing of development have been identified (i.e., posterior tracts tend to mature earlier than anterior and association tracts) (Lebel et al., 2008; Lebel et al., 2010; Krogsrud et al., 2016; Simmonds et al., 2014). Regarding the corpus callosum (CC), the primary interhemispheric commissure of the brain, an overall anterior-to-posterior maturation pattern has been reported in children (Giedd et al., 1999; Thompson et al., 2000). Further, evidence exists for differential timing of white matter microstructural development in boys and girls (Eluvathingal et al., 2007; Clayden et al., 2012; Simmonds et al., 2014; Paus, 2010). In general, girls show earlier overall reductions in MD (Clayden et al., 2012) and boys have a more prolonged growth of white matter microstructure than girls (Simmonds et al., 2014). However, some studies, usually not including adolescence, did not find differences in age associations with white matter microstructure by sex (Muftuler et al., 2012; Krogsrud et al., 2016). The literature about the white matter microstructure differences between right- and left-handed individuals is scarce. In general, studies in adults have shown that left-handed individuals have higher FA and lower MD in several regions compared to right-handed individuals, mainly involving the CC and frontal areas (Westerhausen et al., 2004; McKay et al., 2017).

Substantial work has also detailed how various facets of cognition develop as children grow (Luciana, 2013; Crone and Elzinga, 2015). Importantly, DTI-derived metrics are not only sensitive to age-related changes, but also to cognition, often labeled structure-function associations. For example, multiple studies have shown that FA and MD are related to general intellectual (Clayden et al., 2012; Krogsrud et al., 2016; Simmonds et al., 2014; Muetzel et al., 2015; Nagy et al., 2004; Schmithorst et al., 2005; Peters et al., 2014; Chiang et al., 2009) and motor abilities (Muetzel et al., 2008; Grohs et al., 2018), independent of age and sex. Regarding motor function, performance on a bimanual finger tapping task, which consists on tapping a button as quickly as possible, in adolescents was positively associated with FA in the splenium, the posterior part of the corpus callosum (Muetzel et al., 2008), which integrates interhemispheric signals from the occipital lobes (Schmahmann, 2009). The association between FA in the splenium and motor performance was independent of the higher FA in this CC region due to age. In preschoolers, white matter microstructure of specific locations along the corpus callosum and the corticospinal tract (CST), which controls primary motor activity (Van Wittenberghe and Peterson, 2020), were related to motor skills (Grohs et al., 2018). Contrary to cognitive function, which has shown global associations with white matter microstructure in many tracts of the brain (Muetzel et al., 2015), motor function research in children has been limited to the corpus callosum and the CST. Since motor function, and particularly performance on finger tapping tasks, involves a distributed neural network that depends on the development of neuronal myelination (Bartzokis et al., 2010), it is crucial to explore the associations with other tracts that connect several regions of the brain.

In addition, previous studies in this field have generally been performed using relatively small samples, and are often poorly representative of the general population (e.g., participants with higher SES, higher IQ). Therefore, the results of this type of studies are difficult to generalize. In fact, a study has recently demonstrated that using low representative samples in neuroimaging research has an impact on the associations observed between age and brain structure (LeWinn et al., 2017).

To address the research gap on global white matter microstructure associations with motor function and the potential for expanding upon generalizability of previous studies, we examined how white matter microstructure in the forceps major and minor, and 5 bilateral tracts (cingulum, corticospinal, inferior and superior longitudinal fasciculi, and uncinate) is related to age, sex, handedness and motor ability, measured with a finger tapping task, in a large, population-based sample of children. Given previous research on the development of white matter microstructure, we hypothesized age to be positively associated with FA and negatively associated with MD. Further, though the literature is sparse, we hypothesized that girls would show lower MD values than boys, we expected to find more mature association tracts in girls than in boys, and no age-sex interactions. Based on the literature of handedness in adults, we expected to find higher FA and lower MD values in left-handed children, as compared to right-handed children, specifically in the CC. Lastly, we hypothesized performance on the finger tapping task to be positively associated with FA and negatively with MD, independent of age, sex and handedness, not only in the posterior callosal fibers and the CST, but also in other tracts.

2. Methods

2.1. Participants

The current study is part of the Generation R Study (n = 9901), a population-based cohort based in Rotterdam, the Netherlands (Kooijman et al., 2016). This cohort largely reflects the ethnically diverse background of the population of Rotterdam, although the percentages of mothers from ethnic minorities and lower socioeconomic status are slightly lower in our sample compared to what is expected from the eligible population (Jaddoe et al., 2006). Between March 2013 and November 2015, a neuroimaging assessment was conducted as part of the age-10 assessment visit (White et al., 2018). A total of 3992 children received a brain MRI scan. Of those, 322 (8%) did not complete the diffusion imaging scan. We excluded 271 (7%) participants with completed DTI scan because, as part of the initial pilot phase of the study, their scans were collected with different scanning parameters (e.g., scanner software version), which significantly affected DTI scalar metrics. In addition, the scans of 358 (9%) children were excluded due to poor data or image preprocessing quality. Finally, we excluded ten participants with substantial incidental findings on their MRI scans (Muetzel et al., 2019). The final sample consisted of 3031 children with usable DTI data. The flow chart depicted in Fig. 1 illustrates these exclusions in detail.

The Medical Ethics Committee of the Erasmus Medical Center approved all study procedures, and all parents and children provided written informed consent and assent, respectively. The datasets generated and/or analyzed during the current study are not publicly available due to legal and ethical regulations, but may be made available upon request to the Director of the Generation R Study, Vincent Jaddoe (v.jaddoe@erasmusmc.nl), in accordance with the local, national, and European Union regulations. The code used in this study is available upon request to the first author, Mónica López-Vicente (m.lopez-vicente@erasmusmc.nl).

2.2. Finger tapping task

Motor performance was measured during the age-10 assessment visit using a computerized finger-tapping task. The task was programmed in Python using modules from the PsychoPy toolbox (version 1.90.3)

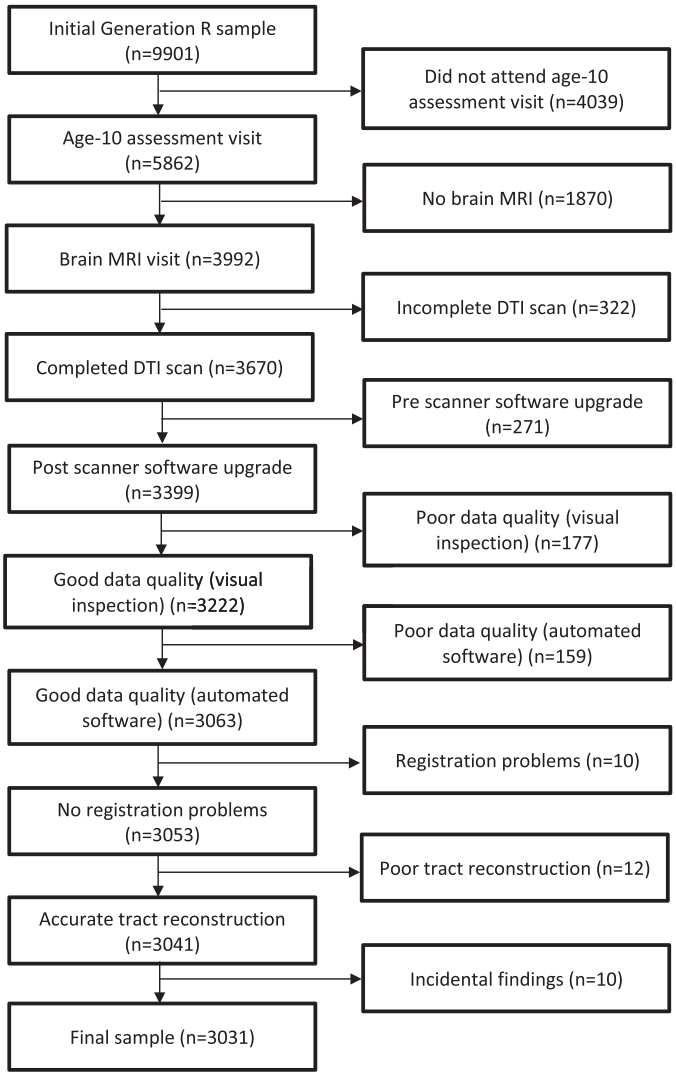

Fig. 1. Flow chart indicating participant inclusion and exclusion from the study population. In total, 6870 Generation R children were not part of these analyses.

(Peirce, 2008). Children were instructed to tap a button as quickly as possible in intervals of 10 seconds. The task consisted of five trials across three conditions: right hand, left hand, and alternating. The inter-trial interval also lasted 10 seconds. Responses were recorded using the bottom right (right hand) and left (left hand) response keys from a Cedra RB834 response box (Cedrus Corporation, San Pedro, CA). For right- and left-hand conditions, two trials were run and we calculated the mean number of taps of both same-hand trials. Trial order was rotated as follows: Right, Left, Alternating, Right, Left. Trials with less than 20 taps were treated as missings.

2.3. Image acquisition

The full image acquisition protocol has been described in detail elsewhere (White et al., 2018). Data were acquired on a study-dedicated 3 Tesla General Electric scanner (GE, MR750W, Milwaukee, WI) using an 8-channel receive-only head coil. Diffusion MRI data were collected with 3 b=0 volumes and 35 diffusion directions using an echo planar imaging sequence (T_R = 12,500 ms, T_E = 72 ms, Field of view = 240 mm x 240 mm, Acquisition Matrix = 120 × 120, slice thickness = 2 mm, number of slices = 65, Asset Acceleration Factor = 2, b = 900 s/mm^2).

2.5. Diffusion image preprocessing

The image preprocessing that we performed on our data has been previously described (Muetzel et al., 2015). Data were converted from DICOM to single file NIfTI format using the dcm2nii tool from the MRIcron library (http://people.cas.sc.edu/rorden/mricron/dcm2nii.html). Data were processed using the Functional MRI of the Brain's Software Library (Jenkinson et al., 2012) and the Camino Diffusion MRI Toolkit (Cook et al., 2006). Image processing tools were executed in Python (version 2.7) through the Neuroimaging in Python Pipelines and Interfaces package (Gorgolewski et al., 2011). Non-brain tissue was removed using the FSL Brain Extraction Tool (Smith, 2002) and images were adjusted for motion and eddy-current induced artifacts (Haselgrove and Moore, 1996) using the FSL "eddy_correct" tool (Jenkinson and Smith, 2001). The resulting transformation matrices were then used to rotate the gradient direction table, in order to account for the rotations applied to the image data (Leemans and Jones, 2009; Jones and Cercignani, 2010). Prior to tensor fitting, data were smoothed using a 2mm median filter to minimize noise (Nucifora et al., 2012). The diffusion tensor was fit using the RESTORE method implemented in Camino (Chang et al., 2005), and common scalar maps (i.e., FA, MD, AD, RD) were then computed. For visual comparison purposes, FA images for 6 randomly selected subjects are shown in Figure S1.

Fully automated probabilistic fiber tractography was performed using the FSL plugin "AutoPtx" (http://fsl.fmrib.ox.ac.uk/fsl/fslwiki/AutoPtx) (de Groot et al., 2015). The method generates subject-specific, probabilistic representations of multiple white matter fiber bundles. The tracts used in the current analyses include: the forceps major and minor; and the bilateral cingulum bundles (CB), corticospinal tracts (CST), inferior and superior longitudinal fasciculi (ILF and SLF), and uncinate fasciculi (UF) (Figure S2). The anatomy and function of these tracts have been well-described in the literature (Schmahmann et al., 2007) and they have shown to have associations with age (Lebel and Beaulieu, 2011), sex (Clayden et al., 2012), and cognitive functions in children (Muetzel et al., 2015).

2.5. Image quality assurance

Raw image quality was assessed through both visual inspection and automated software, as previously described (Muetzel et al., 2015). For the visual inspection, maps of the sum of squares error (SSE) of the tensor fit were inspected for structured signal that is consistent with motion and other artifacts in the diffusion-weighted images (e.g., attenuated slices in diffusion-weighted images), and datasets determined to be of poor quality were excluded (n = 177, 4%). In addition to this visual inspection, slice-wise signal intensity was examined for attenuation resulting from motion, cardiac pulsation and other artifacts using the automated DTIprep quality control tool (http://www.nitrc.org/projects/dtiprep/). An additional 159 (4%) datasets were excluded based on poor quality determined from the DTIprep results.

Probabilistic tractography data were inspected visually in two ways. First, we inspected the native space FA map to FMRIB-58 FA space nonlinear registration to ensure images were all properly aligned to the template. Second, all tracts were visualized to ensure accurate path reconstruction. Ten datasets were excluded due to registration problems and twelve were excluded due to poor reconstruction.

2.6. Covariates

Date of birth, used to calculate the age at the time of the MRI, and sex were determined from medical records obtained at birth. Child ethnicity was defined based on the country of birth of the parents and was coded into three categories (Dutch, non-western, and other western). Non-western category included Cape Verdian, Moroccan, Dutch Antilles, Surinamese, Turkish, African, American and Asian, and other western

category included Indonesian, American and Asian (western), European, and Oceanie. If one of the parents was born in the Netherlands and the other abroad, the country of the non-Dutch parent counted. If both parents were born abroad, the country of the mother determined child ethnicity (Statistics Netherlands, 2004). Maternal education level and household income, proxies of socioeconomic status, were assessed by questionnaire during pregnancy. The Edinburgh Handedness Inventory (EHI) was administered at age 10 years to determine hand preference (Oldfield, 1971). The EHI contains items related to hand use of 10 items, including writing, drawing, throwing, using scissors, and tooth brushing. The laterality quotient obtained from these items ranges from -1 (extreme left-handedness) to +1 (extreme right-handedness). We classified children as right- (quotient > 0) or left-handed (quotient <= 0).

2.7. Statistical analysis

Statistical analyses were conducted using the R Statistical Software (version 3.6.0) (R Core Team, 2014). Global ("whole-brain") DTI metrics were computed for FA and MD by combining scalar values across multiple tracts into a single latent factor, one for each metric, using a confirmatory factor analysis implemented by the Lavaan package (Rosseel, 2012). The details of this approach have been described extensively elsewhere (Muetzel et al., 2015).

We used multiple linear regression models to test the association of age, sex, handedness, and motor performance with white matter microstructure. For age-, sex-, and handedness-associations with white matter microstructure, DTI variables (global metrics, FA, MD, AD, and RD values for the different tracts, separately for right and left hemispheres) were used as outcomes. Age was centered so that the intercept represents the average DTI metric at the mean age of the sample. Age models were adjusted for sex and ethnicity. For sex, boys were used as the reference category. These models were adjusted for age and ethnicity. We also tested whether there were differential age associations in boys and girls by adding an interaction term of age-by-sex into the regression model. For handedness, the right-handed group was used as reference. We adjusted these models for age, sex, and ethnicity. For motor associations with white matter microstructure, finger-tapping performance (number of taps in each condition: right hand, left hand, and alternating) was the outcome. These models were adjusted for age, sex, ethnicity, and handedness (continuous quotient). Note, for all analyses, alongside unstandardized coefficients, standardized regression coefficients are presented so that comparisons can be made across tracts and DTI metrics when considering the magnitude of associations. We generated images of the tracts color-coded based on the age and sex association coefficients using Freeview (https://github.com/muet0005/YNIMG_117643).

Given the number of statistical tests examined with individual tracts, a false discovery rate (FDR) correction was separately applied to each analysis (age, sex, handedness, right hand, left hand and alternating finger tapping task) to control for Type-I error (Benjamini and Hochberg, 1995). Associations with $p_{corrected} < 0.05$ were considered significant. In total, 12 tracts with FA, MD, AD, and RD were tested for age associations, resulting in 48 tests for age, plus the two global metrics. Another 50 tests were run for sex differences, and 50 test more for handedness. In addition, the 12 tracts, four DTI metrics and two global metrics were also associated across 3 conditions of the finger tapping task, resulting in 50 tests for each of the condition.

2.8. Missing data

We performed multiple imputations of missing values in covariates and finger tapping task among all participants of the initial sample. We used the mice (multiple imputation by chained equations) R package (van Buuren and Groothuis-Oudshoorn, 2011). With 60 iterations, a total of 40 imputed datasets were generated, and results were pooled using Rubin's rules (Rubin, 2004).

2.9. Non-response analysis

The specific sample included in these analyses was not completely representative of the original cohort due to the loss of follow up (White et al., 2018). Children included in this analysis ($n = 3031$) were more likely to have parents from a higher socioeconomic position compared to children that were not included in the analyses ($n = 6870$). In order to adjust for potential selection bias (e.g., certain portions of the sample being underrepresenting in statistical models), we implemented inverse probability weighting (IPW) in linear regression models (Weisskopf et al., 2015). We used child ethnicity, maternal education, and household income variables to calculate the weights. As sensitivity analyses, we also ran the main regression models without applying the IPW.

3. Results

3.1. Sample characteristics

Table 1 outlines child and maternal characteristics of the current sample. It was equally distributed by sex, the mean age was 10 years old (range = 8–12, SD=0.6), and sixty percent were of Dutch origin. In general, right hand preference was higher in the sample (laterality quotient mean=0.71, SD=0.51). For right-handed children ($n = 2646$), the performance on the finger tapping task was slightly better with the right hand (the mean number of taps was 42 in this condition, while it was around 38 in the other two conditions). For left-handed children ($n = 293$), the opposite pattern was observed. There were no large differences in age and performance between boys and girls. In general, the mean number of taps was one point higher in boys than in girls.

3.2. DTI metrics

The observed values of FA, MD, AD, and RD for each tract are shown in Fig. 2 and Supplementary Figs 3–5. The scatter plots indicated positive relationships between FA and age, which were consistent across different tracts, though relatively small in magnitude. Boys showed higher FA values than girls in the cingulum bundles, while girls showed higher FA in the inferior longitudinal fasciculi. The highest FA values were observed in a tract that showed no relationship with age, the forceps minor. MD values were negatively related to age. Girls showed lower MD in forceps major, as well as in the inferior and the superior longitudinal fasciculi than boys. The values of AD were generally higher in boys than in girls, but no clear relationships with age were observed. The higher AD values were observed in the forceps major and the forceps minor. In general, RD values were negatively related to age. Boys had higher RD in the forceps major and in the inferior longitudinal fasciculi.

3.3. Age and white matter

Age was positively associated with global FA (coefficient=0.340; 95%CI=0.231, 0.449) and negatively with global MD (coefficient=-0.050; 95%CI=-0.062, -0.037). For all tracts, except the FMi, age was positively related to FA and negatively related to MD after adjusting for sex and ethnicity (Table 2). Specifically, the FA values increased between 0.001 and 0.009 every year in our sample, while the MD decreased by 0.022 and 0.069 10^{-4} mm^2/s every year. Both AD and RD were mostly negatively related to age. However, no associations were observed with AD in the bilateral CB and CST, the FMa, the right UF, and RD in the FMi (Table 3). Fig. 3 displays each tract color-coded based on the coefficients for age. Globally, the stronger associations were observed in the FMa and the bilateral CB and SLF. These results were similar without applying IPW (Tables S1 and S2).

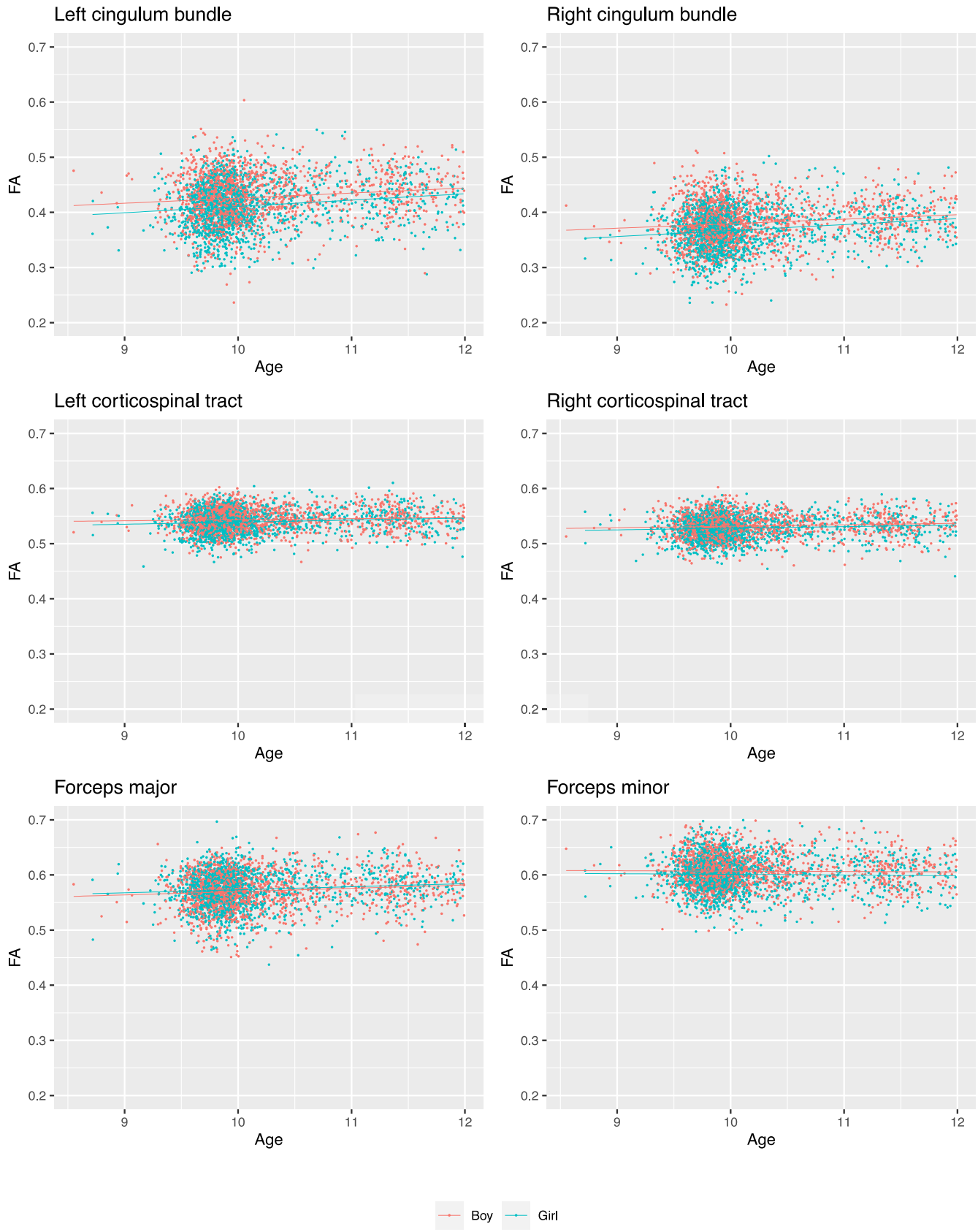

Fig. 2. Scatter plots of FA values in each tract and age by sex.

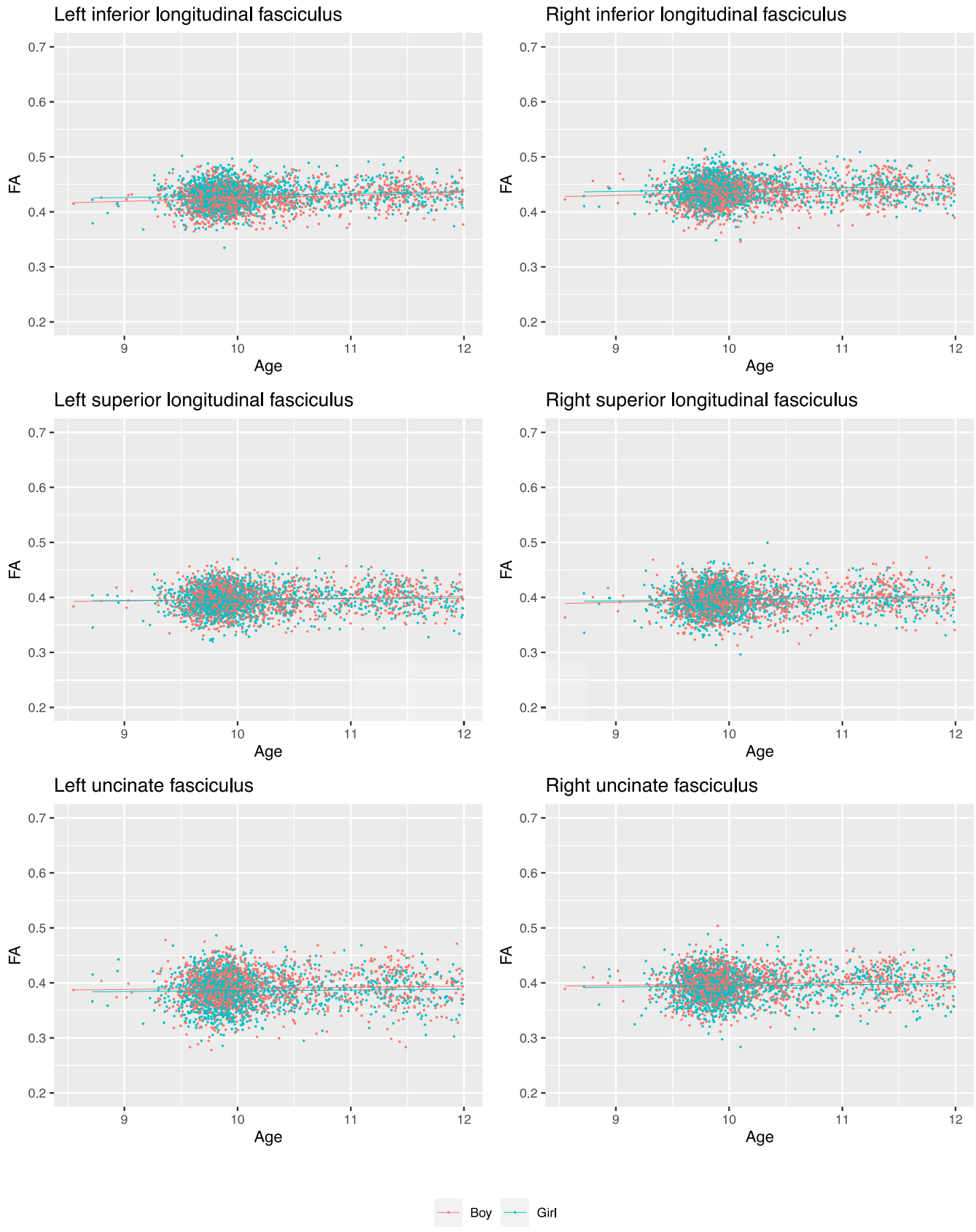

Fig. 2. Continued

Table 1
Sample characteristics. [a]Age ranges from 8.6 to 12.0 years old; [b]The laterality quotient ranges from -1 (extreme left-handedness) to +1 (extreme right-handedness); [c]The number of taps with the right hand ranges from 20 to 62 taps; [d]The number of taps with the left hand ranges from 20 to 59; [e]The number of taps in the alternating trial ranges from 20 to 99. The percentages of missing values were 2% for ethnicity, 3% for handedness, 6% right hand finger tapping, 6% left hand finger tapping, 13% alternating finger tapping, 8% for maternal education and 22% for household income.

N		Full Sample 3031	Girls 1526	Boys 1505
Child variables				
Age at MRI visit, years (mean, SD)[a]		10.15 ± 0.60	10.11 ± 0.57	10.19 ± 0.62
Ethnicity (n, %)				
	Dutch	1862 (61)	940 (62)	922 (61)
	Non-Western	847 (28)	409 (27)	438 (29)
	Other Western	267 (9)	147 (10)	120 (8)
Handedness, laterality quotient (mean, SD)[b]		0.71 ± 0.51	0.71 ± 0.49	0.71 ± 0.52
Right-handed (n = 2646)				
Finger tapping, right hand, number of taps (mean, SD)[c]		42.09 ± 5.83	41.87 ± 5.78	42.32 ± 5.87
Finger tapping, left hand, number of taps (mean, SD)[d]		38.32 ± 5.20	37.60 ± 5.00	39.06 ± 5.31
Finger tapping, alternating, number of taps (mean, SD)[e]		38.33 ± 10.54	37.61 ± 10.18	39.07 ± 10.85
Left-handed (n = 293)				
Finger tapping, right hand, number of taps (mean, SD)[c]		38.72 ± 5.10	38.12 ± 5.10	39.25 ± 5.04
Finger tapping, left hand, number of taps (mean, SD)[d]		42.89 ± 5.71	42.49 ± 6.02	43.25 ± 5.42
Finger tapping, alternating, number of taps (mean, SD)[e]		40.87 ± 11.22	41.48 ± 11.37	40.32 ± 11.08
Maternal variables				
Education (n, %)				
	Higher	1500 (49)	742 (49)	758 (50)
	Secondary	1111 (37)	577 (38)	534 (35)
	Primary	179 (6)	93 (6)	86 (6)
Household netto income (n, %)				
	High (>2200€)	1514 (50)	785 (51)	729 (48)
	Medium (1200€-2200€)	533 (18)	249 (16)	284 (19)
	Low (<1200€)	310 (10)	159 (10)	151 (10)

Table 2
Age associations with major white matter fiber bundles (FA and MD). Linear regression models adjusted for sex and ethnicity. Multiple imputation and inverse probability weighting were applied. Hemispheres: L=left; R=right. DTI metrics: FA=Fractional anisotropy; MD=Mean diffusivity. Tracts: CB=Cingulum bundle; CST=Corticospinal tract; FMa=Forceps major; FMi=Forceps minor; ILF=Inferior longitudinal fasciculus; SLF=Superior longitudinal fasciculus; UF=Uncinate fasciculus.

DTI metrics	Tract	Hemisphere	Coefficient	95%CI		Standardized coefficient	p	p_{FDR}
				Lower	Upper			
FA	Global	–	0.340	0.231	0.449	0.113	<0.001	<0.001
	CB	L	0.009	0.007	0.012	0.128	<0.001	<0.001
		R	0.009	0.007	0.012	0.128	<0.001	<0.001
	CST	L	0.003	0.002	0.004	0.142	<0.001	<0.001
		R	0.003	0.001	0.004	0.083	<0.001	<0.001
	FMa	–	0.005	0.003	0.007	0.079	<0.001	<0.001
	FMi	–	−0.001	−0.003	0.001	0.094	0.272	0.290
	ILF	L	0.004	0.003	0.006	−0.020	<0.001	<0.001
		R	0.004	0.002	0.005	0.123	<0.001	<0.001
	SLF	L	0.002	0.001	0.003	0.102	0.005	0.007
		R	0.003	0.002	0.005	0.052	<0.001	<0.001
	UF	L	0.001	0.000	0.003	0.083	0.128	0.149
		R	0.002	0.001	0.004	0.028	0.006	0.008
MD	Global	–	−0.050	−0.062	−0.037	−0.135	<0.001	<0.001
	CB	L	−0.057	−0.075	−0.040	−0.117	<0.001	<0.001
		R	−0.067	−0.085	−0.050	−0.142	<0.001	<0.001
	CST	L	−0.051	−0.081	−0.021	−0.070	0.001	0.002
		R	−0.055	−0.085	−0.025	−0.076	0.001	0.001
	FMa	–	−0.068	−0.107	−0.029	−0.062	0.001	0.002
	FMi	–	−0.012	−0.031	0.007	−0.023	0.210	0.228
	ILF	L	−0.059	−0.074	−0.043	−0.130	<0.001	<0.001
		R	−0.053	−0.072	−0.034	−0.098	<0.001	<0.001
	SLF	L	−0.065	−0.079	−0.051	−0.167	<0.001	<0.001
		R	−0.069	−0.085	−0.053	−0.156	<0.001	<0.001
	UF	L	−0.034	−0.047	−0.021	−0.098	<0.001	<0.001
		R	−0.022	−0.035	−0.009	−0.060	0.001	0.002

3.4. Sex differences in white matter

Girls showed lower global MD than boys (coefficient=-0.076; 95%CI=-0.091, -0.061), while global FA was not associated with sex. Girls and boys differed in FA in all tracts except for the SLF, after adjusting for age and ethnicity (Table 4). Girls showed higher FA in the bilateral ILF and in the FMa, whereas boys showed higher FA in the CB, CST, FMi, and the UF. Girls and boys also differed in MD, with girls showing lower MD in all tracts, except the FMi, the right CST, and the UF. AD was lower in girls in most of the tracts. In girls, RD was lower in FMa, ILF, and SLF tracts than in boys, and higher in the left CB, and FMi (Table 5). Fig. 4 displays each tract color-coded based on the coefficient

Table 3
Age associations with major white matter fiber bundles (AD and RD). Linear regression models adjusted for sex and ethnicity. Multiple imputation and inverse probability weighting were applied. Hemispheres: L=left; R=right. DTI metrics: AD=Axial diffusivity; RD=Radial diffusivity. Tracts: CB=Cingulum bundle; CST=Corticospinal tract; FMa=Forceps major; FMi=Forceps minor; ILF=Inferior longitudinal fasciculus; SLF=Superior longitudinal fasciculus; UF=Uncinate fasciculus.

DTI metrics	Tract	Hemisphere	Coefficient	95%CI		Standardized coefficient	p	p_{FDR}
				Lower	Upper			
AD	CB	L	0.023	−0.009	0.054	0.025	0.160	0.178
		R	0.005	−0.025	0.035	0.006	0.745	0.760
	CST	L	−0.063	−0.151	0.025	−0.030	0.160	0.178
		R	−0.079	−0.165	0.008	−0.039	0.075	0.092
	FMa	–	−0.035	−0.078	0.007	−0.030	0.102	0.121
	FMi	–	−0.043	−0.076	−0.010	−0.046	0.011	0.014
	ILF	L	−0.033	−0.055	−0.010	−0.052	0.004	0.006
		R	−0.033	−0.058	−0.007	−0.046	0.011	0.014
	SLF	L	−0.074	−0.091	−0.057	−0.147	<0.001	<0.001
		R	−0.065	−0.084	−0.047	−0.124	<0.001	<0.001
	UF	L	−0.034	−0.054	−0.013	−0.060	0.001	0.002
		R	−0.006	−0.027	0.015	−0.011	0.555	0.578
RD	CB	L	−0.097	−0.121	−0.074	−0.149	<0.001	<0.001
		R	−0.104	−0.125	−0.082	−0.173	<0.001	<0.001
	CST	L	−0.045	−0.058	−0.032	−0.124	<0.001	<0.001
		R	−0.043	−0.057	−0.030	−0.115	<0.001	<0.001
	FMa	–	−0.084	−0.125	−0.044	−0.074	<0.001	<0.001
	FMi	–	0.003	−0.019	0.026	0.005	0.767	0.767
	ILF	L	−0.072	−0.089	−0.054	−0.148	<0.001	<0.001
		R	−0.063	−0.083	−0.043	−0.113	<0.001	<0.001
	SLF	L	−0.061	−0.077	−0.045	−0.136	<0.001	<0.001
		R	−0.071	−0.089	−0.053	−0.140	<0.001	<0.001
	UF	L	−0.034	−0.052	−0.017	−0.072	<0.001	<0.001
		R	−0.029	−0.045	−0.013	−0.066	<0.001	0.001

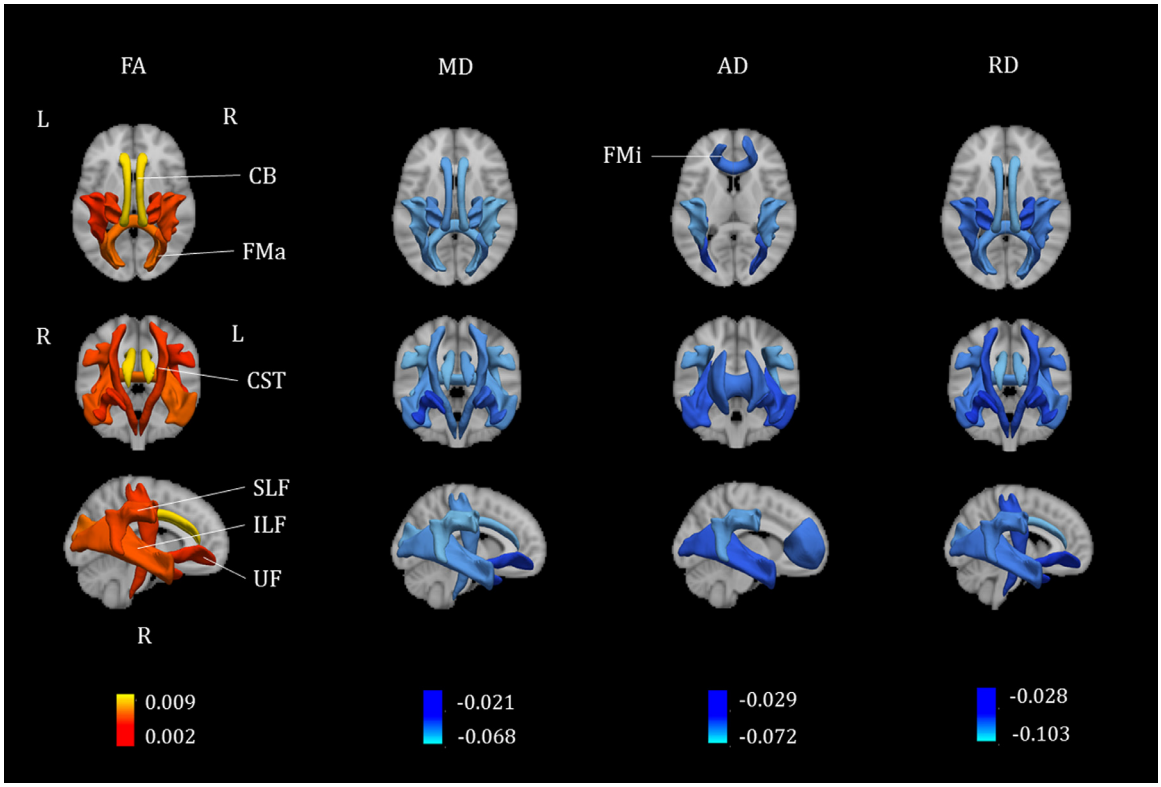

Fig. 3. Age associations with FA, MD, AD, and RD in the major white matter fiber bundles. Linear regression models adjusted for sex and ethnicity. Multiple imputation and inverse probability weighting were applied. Lighter color indicates higher association coefficients. Only the tracts showing associations with $p < 0.05$ are represented. Hemispheres: L=left; R=right. DTI metrics: AD=Axial diffusivity; FA=Fractional anisotropy; MD=Mean diffusivity; RD=Radial diffusivity. Tracts: CB=Cingulum bundle; CST=Corticospinal tract; FMa=Forceps major; FMi=Forceps minor; ILF=Inferior longitudinal fasciculus; SLF=Superior longitudinal fasciculus; UF=Uncinate fasciculus.

Table 4
Sex differences in major white matter fiber bundles (FA and MD). Linear regression models adjusted for age and ethnicity. Reference group = boys. Multiple imputation and inverse probability weighting were applied. Hemispheres: L=left; R=right. DTI metrics: FA=Fractional anisotropy; MD=Mean diffusivity. Tracts: CB=Cingulum bundle; CST=Corticospinal tract; FMa=Forceps major; FMi=Forceps minor; ILF=Inferior longitudinal fasciculus; SLF=Superior longitudinal fasciculus; UF=Uncinate fasciculus.

DTI metrics	Tract	Hemisphere	Coefficient	95%CI		Standardized coefficient	p	p_{FDR}
				Lower	Upper			
FA	Global	–	−0.111	−0.241	0.019	−0.031	0.094	0.118
	CB	L	−0.014	−0.017	−0.011	−0.163	<0.001	<0.001
		R	−0.011	−0.014	−0.008	−0.142	<0.001	<0.001
	CST	L	−0.004	−0.006	−0.003	−0.105	<0.001	<0.001
		R	−0.004	−0.005	−0.002	−0.087	<0.001	<0.001
	FMa	–	0.003	0.001	0.005	0.045	0.014	0.019
	FMi	–	−0.006	−0.008	−0.004	−0.097	<0.001	<0.001
	ILF	L	0.005	0.003	0.006	0.115	<0.001	<0.001
		R	0.006	0.004	0.007	0.129	<0.001	<0.001
	SLF	L	−0.001	−0.003	0.001	−0.021	0.255	0.289
		R	0.001	−0.001	0.002	0.012	0.528	0.562
	UF	L	−0.005	−0.007	−0.003	−0.081	<0.001	<0.001
		R	−0.004	−0.006	−0.002	−0.076	<0.001	<0.001
MD	Global	–	−0.076	−0.091	−0.061	−0.172	<0.001	<0.001
	CB	L	−0.055	−0.076	−0.034	−0.095	<0.001	<0.001
		R	−0.054	−0.074	−0.034	−0.095	<0.001	<0.001
	CST	L	−0.050	−0.087	−0.014	−0.058	0.007	0.010
		R	0.000	−0.037	0.036	−0.001	0.979	0.979
	FMa	–	−0.155	−0.201	−0.108	−0.118	<0.001	<0.001
	FMi	–	0.001	−0.021	0.023	0.002	0.934	0.953
	ILF	L	−0.119	−0.138	−0.100	−0.220	<0.001	<0.001
		R	−0.156	−0.179	−0.133	−0.240	<0.001	<0.001
	SLF	L	−0.101	−0.118	−0.085	−0.217	<0.001	<0.001
		R	−0.119	−0.138	−0.100	−0.224	<0.001	<0.001
	UF	L	−0.012	−0.028	0.003	−0.030	0.108	0.131
		R	−0.016	−0.031	0.000	−0.037	0.047	0.062

for sex. Adding an interaction term of age-by-sex into the regression model was not significant for any tract (all $p_{corrected} > 0.2$). These results were similar without applying IPW (Tables S3 and S4).

3.5. Handedness differences in white matter

Handedness was not associated with white matter microstructure in any tract after FDR correction. Before correcting for multiple testing, left-handed children showed lower FA and higher RD in the left CST and left SLF, as compared to right-handed children (Tables S5 and S6). The results were very similar without applying IPW (Tables S7 and S8).

3.6. Motor performance

FA in the FMa was positively associated with right-hand finger tapping performance after adjusting for age, sex, ethnicity, and handedness (Table 6). Further, MD and RD in the FMa were negatively related to right-hand finger tapping performance (Tables 6 and 7). Global FA and FA of other tracts, such as the CB, the CST, and the right SLF, were positively associated with this task, but only before FDR correction (Table 6). Similar results were observed for left-hand finger tapping task, but no association survived FDR correction (Tables S9 and S10). Lastly, alternating finger tapping performance was not associated with FA and diffusivity measures in any tract (Tables S11 and S12). All the results were similar without applying IPW (Tables S13–S18).

4. Discussion

This study represents one of the largest investigations of age, sex, handedness, and motor performance associations with white matter microstructure in children. Using data from a single, study-dedicated scanner, we showed white matter microstructural associations with age, sex and motor performance in children aged 8–12 years from the general population. Age was positively associated with FA and negatively with MD in almost all white matter tracts. Further, girls showed lower global MD and higher FA than boys in tracts that tend to develop later. No remarkable differences were observed in white matter microstructure between right- and left-handed children. Lastly, previous work examining the association between bimanual task performance and corpus callosum microstructure was replicated in a larger and population-based sample of children. The white matter FA of other tracts, such as the CB, the CST, and the right SLF, was only associated with better motor function before multiple testing correction.

This study demonstrates robust associations between age and white matter microstructure in children ages 8-to-12 years. Consistent with previous work (Lebel et al., 2008; Eluvathingal et al., 2007; Barnea-Goraly et al., 2005; Clayden et al., 2012; Lebel et al., 2010; Muftuler et al., 2012; Qiu et al., 2008; Brouwer et al., 2012; Krogsrud et al., 2016; Simmonds et al., 2014; Cascio et al., 2007; Lebel et al., 2019; Tamnes et al., 2018), multiple white matter tracts showed age-related associations with DTI scalar metrics. All tracts except for the forceps minor, the anterior callosal fibers, showed positive age associations with FA and negative associations with MD. Both RD and AD showed mostly negative associations with age, being RD age coefficients considerably larger than AD. Thus, the age-related differences that we identify may suggest continued myelination and/or axonal packing over a narrow age range in children (Eluvathingal et al., 2007). The non-overlapping confidence intervals of the age association coefficients of forceps minor and forceps major also suggested that these two tracts have different developmental patterns (i.e., they may develop at different rates or points in time). The lack of an association in the forceps minor is loosely in line with previous work showing that the fastest growth in the anterior areas of the corpus callosum occurred at ages 3 to 6 years (Giedd et al., 1999; Thompson et al., 2000), suggesting age associations would be more apparent in this tract at earlier ages.

Differences in white matter development between boys and girls have been reported previously (Eluvathingal et al., 2007; Clayden et al., 2012; Simmonds et al., 2014). In particular, earlier development of

Table 5
Sex differences in major white matter fiber bundles (AD and RD). Linear regression models adjusted for age and ethnicity. Reference group = boys. Multiple imputation and inverse probability weighting were applied. Hemispheres: L=left; R=right. DTI metrics: AD=Axial diffusivity; RD=Radial diffusivity. Tracts: CB=Cingulum bundle; CST=Corticospinal tract; FMa=Forceps major; FMi=Forceps minor; ILF=Inferior longitudinal fasciculus; SLF=Superior longitudinal fasciculus; UF=Uncinate fasciculus.

DTI metrics	Tract	Hemisphere	Coefficient	95%CI		Standardized coefficient	*p*	p_{FDR}
				Lower	Upper			
AD	CB	L	−0.256	−0.294	−0.218	−0.236	<0.001	<0.001
		R	−0.208	−0.244	−0.172	−0.204	<0.001	<0.001
	CST	L	−0.162	−0.268	−0.057	−0.065	0.003	0.004
		R	−0.022	−0.125	0.082	−0.009	0.679	0.708
	FMa	–	−0.210	−0.261	−0.159	−0.146	<0.001	<0.001
	FMi	–	−0.099	−0.138	−0.059	−0.090	<0.001	<0.001
	ILF	L	−0.130	−0.157	−0.103	−0.171	<0.001	<0.001
		R	−0.182	−0.213	−0.152	−0.212	<0.001	<0.001
	SLF	L	−0.167	−0.188	−0.147	−0.278	<0.001	<0.001
		R	−0.188	−0.210	−0.167	−0.298	<0.001	<0.001
	UF	L	−0.068	−0.092	−0.043	−0.101	<0.001	<0.001
		R	−0.066	−0.091	−0.041	−0.095	<0.001	<0.001
RD	CB	L	0.045	0.017	0.073	0.057	0.002	0.003
		R	0.023	−0.003	0.049	0.032	0.078	0.100
	CST	L	0.006	−0.010	0.022	0.014	0.448	0.487
		R	0.010	−0.006	0.026	0.023	0.213	0.248
	FMa	–	−0.127	−0.176	−0.078	−0.093	<0.001	<0.001
	FMi	–	0.051	0.024	0.078	0.067	<0.001	<0.001
	ILF	L	−0.113	−0.134	−0.093	−0.195	<0.001	<0.001
		R	−0.143	−0.167	−0.119	−0.214	<0.001	<0.001
	SLF	L	−0.068	−0.087	−0.049	−0.127	<0.001	<0.001
		R	−0.084	−0.106	−0.062	−0.138	<0.001	<0.001
	UF	L	0.015	−0.006	0.036	0.026	0.155	0.184
		R	0.009	−0.010	0.028	0.017	0.345	0.383

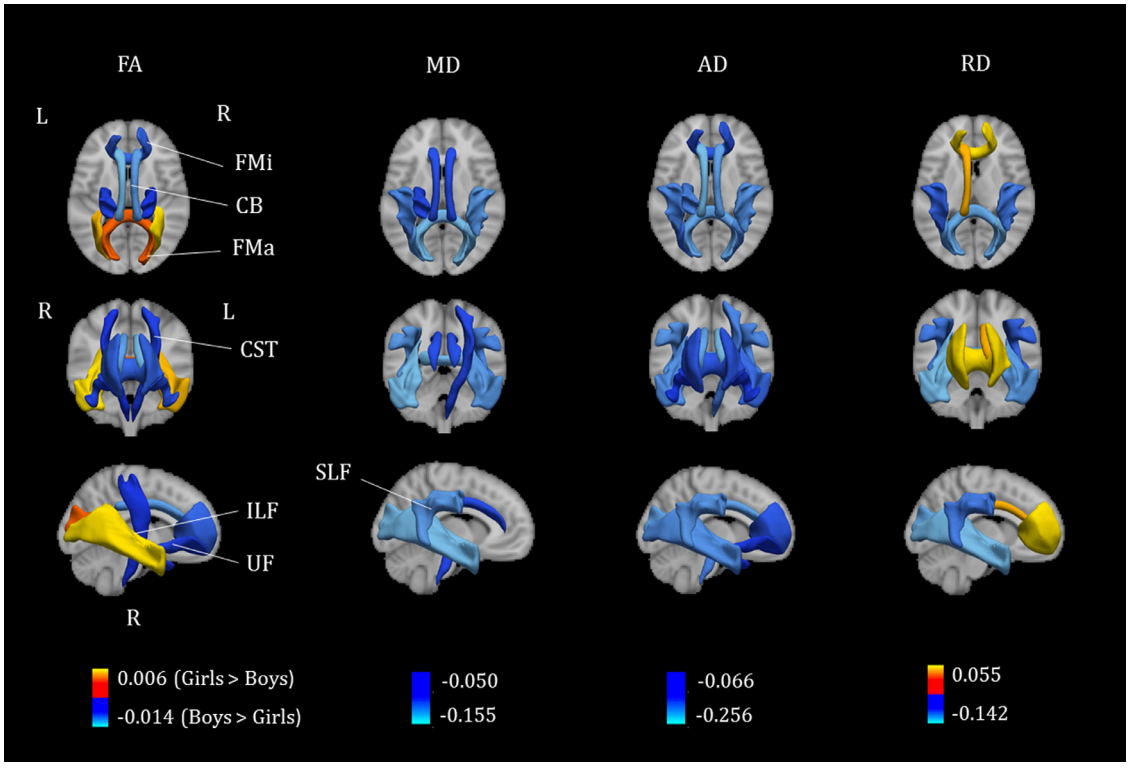

Fig. 4. Sex differences in FA, MD, AD, and RD in the major white matter fiber bundles. Linear regression models adjusted for age and ethnicity. Multiple imputation and inverse probability weighting were applied. Lighter color indicates higher association coefficients. Only the tracts showing associations with $p < 0.05$ are represented. Hemispheres: L=left; R=right. DTI metrics: AD=Axial diffusivity; FA=Fractional anisotropy; MD=Mean diffusivity; RD=Radial diffusivity. Tracts: CB=Cingulum bundle; CST=Corticospinal tract; FMa=Forceps major; FMi=Forceps minor; ILF=Inferior longitudinal fasciculus; SLF=Superior longitudinal fasciculus; UF=Uncinate fasciculus.

Table 6
Associations between major white matter fiber bundles and right–hand finger tapping performance (FA and MD). Linear regression models adjusted for age, sex, ethnicity, and handedness. Multiple imputation and inverse probability weighting were applied. Hemispheres: L=left; R=right. DTI metrics: FA=Fractional anisotropy; MD=Mean diffusivity. Tracts: CB=Cingulum bundle; CST=Corticospinal tract; FMa=Forceps major; FMi=Forceps minor; ILF=Inferior longitudinal fasciculus; SLF=Superior longitudinal fasciculus; UF=Uncinate fasciculus.

DTI metrics	Tract	Hemisphere	Coefficient	95%CI Lower	Upper	Standardized coefficient	p	p_{FDR}
FA	Global	–	0.119	0.001	0.236	0.037	0.048	0.171
	CB	L	5.229	0.199	10.258	0.039	0.042	0.160
		R	5.846	0.405	11.286	0.039	0.035	0.160
	CST	L	11.174	0.877	21.471	0.040	0.034	0.160
		R	12.203	2.068	22.339	0.044	0.018	0.120
	FMa	–	9.720	3.384	16.056	0.055	0.003	0.044
	FMi	–	1.952	−4.724	8.628	0.011	0.567	0.740
	ILF	L	−0.414	−10.380	9.552	−0.002	0.935	0.935
		R	2.778	−6.791	12.347	0.011	0.569	0.740
	SLF	L	5.188	−4.447	14.823	0.020	0.291	0.674
		R	10.657	1.743	19.571	0.043	0.019	0.120
	UF	L	−3.088	−10.304	4.127	−0.016	0.402	0.702
		R	−0.603	−8.757	7.551	−0.003	0.885	0.922
MD	Global	–	−0.231	−1.240	0.778	−0.009	0.653	0.776
	CB	L	−0.434	−1.162	0.294	−0.022	0.242	0.638
		R	−0.633	−1.395	0.129	−0.031	0.104	0.305
	CST	L	−0.087	−0.497	0.323	−0.006	0.678	0.776
		R	0.218	−0.191	0.627	0.016	0.296	0.674
	FMa	–	−0.552	−0.883	−0.221	−0.062	0.001	0.028
	FMi	–	−0.272	−0.958	0.415	−0.014	0.438	0.704
	ILF	L	−0.415	−1.220	0.391	−0.019	0.313	0.681
		R	−0.305	−0.978	0.368	−0.017	0.374	0.696
	SLF	L	−0.256	−1.190	0.679	−0.010	0.592	0.740
		R	−0.582	−1.398	0.234	−0.026	0.163	0.451
	UF	L	0.213	−0.807	1.232	0.008	0.683	0.776
		R	0.448	−0.543	1.440	0.017	0.376	0.696

Table 7
Associations between white matter fiber bundles and right-hand finger tapping performance (AD and RD). Linear regression models adjusted for age, sex, ethnicity, and handedness. Multiple imputation and inverse probability weighting were applied. Hemispheres: L=left; R=right. DTI metrics: AD=Axial diffusivity; RD=Radial diffusivity. Tracts: CB=Cingulum bundle; CST=Corticospinal tract; FMa=Forceps major; FMi=Forceps minor; ILF=Inferior longitudinal fasciculus; SLF=Superior longitudinal fasciculus; UF=Uncinate fasciculus.

DTI metrics	Tract	Hemisphere	Coefficient	95%CI Lower	Upper	Standardized coefficient	p	p_{FDR}
AD	CB	L	0.200	−0.209	0.609	0.019	0.338	0.696
		R	0.053	−0.377	0.483	0.005	0.808	0.878
	CST	L	0.021	−0.121	0.163	0.004	0.770	0.856
		R	0.135	−0.008	0.278	0.028	0.064	0.200
	FMa	–	−0.406	−0.714	−0.098	−0.050	0.010	0.120
	FMi	–	−0.043	−0.433	0.347	−0.004	0.828	0.881
	ILF	L	−0.320	−0.890	0.250	−0.021	0.272	0.674
		R	−0.147	−0.652	0.359	−0.011	0.569	0.740
	SLF	L	0.039	−0.709	0.788	0.002	0.919	0.935
		R	0.162	−0.553	0.877	0.009	0.657	0.776
	UF	L	−0.202	−0.853	0.449	−0.012	0.543	0.740
		R	0.177	−0.450	0.803	0.010	0.581	0.740
RD	CB	L	−0.543	−1.089	0.003	−0.036	0.051	0.171
		R	−0.653	−1.248	−0.059	−0.040	0.031	0.160
	CST	L	−1.198	−2.179	−0.218	−0.044	0.017	0.120
		R	−1.146	−2.098	−0.195	−0.044	0.018	0.120
	FMa	–	−0.531	−0.844	−0.219	−0.062	0.001	0.028
	FMi	–	−0.231	−0.793	0.331	−0.015	0.421	0.702
	ILF	L	−0.260	−1.005	0.486	−0.013	0.495	0.728
		R	−0.309	−0.961	0.344	−0.018	0.354	0.696
	SLF	L	−0.303	−1.101	0.495	−0.014	0.457	0.704
		R	−0.730	−1.430	−0.029	−0.038	0.041	0.160
	UF	L	0.307	−0.432	1.046	0.015	0.416	0.702
		R	0.298	−0.501	1.098	0.013	0.464	0.704

white matter has been observed in girls (Clayden et al., 2012), while boys show larger, more prolonged and continuous white matter microstructural growth (Simmonds et al., 2014; Paus, 2010). Lower MD and AD was generally observed in girls, which may be indicators of earlier development or could be due to lower axonal caliber in comparison to boys (Paus, 2010; Perrin et al., 2008). We observed differences between boys and girls in FA and RD in some tracts. The combination of high FA and low RD suggested that boys had higher myelination in CB, CST, FMi, and UF than girls, while the opposite was found in the FMa and the ILF tracts. Some of these tracts have been previously found to show different developing timing between boys and girls. Specifically, previous studies have reported higher maturation rates of

the ILF in girls between 6 and 17 (Eluvathingal et al., 2007) and between 8 and 16 years old than in boys (Clayden et al., 2012), while FA in the left CST showed a significant growth in boys at same ages, not observed in girls (Clayden et al., 2012). Noteworthy, the tracts that showed higher FA in girls than in boys were association tracts, while tracts like CST or FMi, higher myelinated in boys than in girls, tend to develop earlier in life. In line with other studies (Muftuler et al., 2012; Krogsrud et al., 2016), we did not find age-sex interactions, suggesting similar age-associations with white matter microstructure in boys and girls between 8 and 12 years old. Even though we did not find such an interaction, it may still be present in other developmental stages, such as adolescence (Clayden et al., 2012; Simmonds et al., 2014).

Our results showed no differences in the white matter microstructure between right- and left-handed children after controlling for multiple testing. Previous studies in adults observed higher FA within white matter pathways in left-handed individuals, as compared to right-handed individuals (Westerhausen et al., 2004; McKay et al., 2017). These differences have been linked to the lower asymmetry in left-handed individuals. It has been suggested that the asymmetry depends on both the innate preference of hand use and the early developmental experience (McKay et al., 2017; Andersen and Siebner, 2018). Since the sample of our study are children, the lack of differences in white matter microstructure by handedness preference may be due to either developmental differences between children and adults related to asymmetric brain structure, or due to less accumulated experience that could generate asymmetrical differences between right and left handers. Since the majority of the population is right-handed, many features in the environment are designed for right-handed individuals, such that those who are left-handed often have some level of mixed-dominance. Finally, the small sample size of left-handed participants in comparison to the right-handed group (n=293 vs. n=2646) in our sample decreases our power to detect associations.

Previous work explored the structure-function associations between diffusion metrics and cognitive performance (Muetzel et al., 2015). Specifically, the authors observed associations between global FA and non-verbal IQ, as well as visuospatial ability. The present study reported an association between motor performance and white matter microstructure in the forceps major, the posterior callosal fibers. Together with the associations found between age and white matter microstructure in these tracts, these results suggest that children performing better in the finger tapping task have more mature corpus callosum than those who performed poorly. Importantly, these associations were independent of age, sex, ethnicity, and handedness, suggesting that the variability in the motor task performance related to white matter microstructure was not explained by these other variables. However, the directionality of the associations remains unknown, given the cross-sectional design of the study. Since both finger tapping performance and white matter microstructure were measured at the same time, we were not able to test which of the two variables preceded the other in our data. The association with forceps major is remarkably consistent with previous work using other samples that observed associations between motor function and the corpus callosum (Muetzel et al., 2008; Grohs et al., 2018). Particularly, Muetzel et al. (Muetzel et al., 2008) also reported associations between the FA in the posterior part of corpus callosum and finger tapping performance in a smaller sample ($n = 92$, ages 9–23 years), however in this study the findings were observed with the alternating condition. Regarding the study from Grohs et al. (Grohs et al., 2018), correlations were observed between FA and MD in specific regions of corpus callosum motor fibers, in anterior areas, and motor function in preschoolers. Our findings provide new evidence for the posterior corpus callosum and finger tapping performance associations in a large sample of school-aged children. The weak estimates obtained in other tracts did not support the hypothesis that finger tapping performance could be an indicator of global white matter microstructure.

This study has some limitations. The results might be biased by the interindividual variability due to the cross-sectional design (Crone and Elzinga, 2015). We were not able to test the causality of the associations between motor performance and the DTI metrics because of the design of the study. The narrow age range probably limited our capacity to observe interactions between sex and age. Finally, while largely reflecting the ethnically diverse background of Rotterdam, our cohort was not completely representative and we have encountered non-random loss to follow up. A problem of selection bias usually arises in these scenarios, however, the similarity of the results before and after applying IPW suggests that the impact of selection bias due to loss of follow up was likely minimal in these associations.

The key strength of this study is that it was performed in a fairly representative ethnically diverse population-based cohort with a large sample size. The advantages of studying the brain at the population level as opposed to using small samples include the higher statistical power, the lower bias and the higher generalizability of the results (LeWinn et al., 2017; Paus, 2010; White et al., 2013). The present study utilized a single, study-dedicated MR system, and processed all imaging data using the same pipeline. Regarding the DTI processing, we used a probabilistic tractography approach, which provides native-space information on white matter tracts. In contrast to voxel-based analyses, this method is less sensitive to common problems such as misalignment. An added value of this study was the inclusion of AD and RD to better characterize the origin of the associations with the main DTI metrics, FA and MD.

5. Conclusions

We observed that age was associated with higher FA and lower MD in the main tracts in 3031 children from the general population between 8 and 12 years old. Girls showed lower global MD than boys and higher FA in tracts that tend to develop later and no age-sex interactions were found. No differences were observed in white matter microstructure between right- and left-handed children. White matter FA in forceps major was positively associated with motor performance. These findings support the structure-function associations in a large sample of children. However, our results do not provide evidence for a relationship between finger tapping task performance and global white matter microstructure. Longitudinal studies using large sample sizes that include repeated measures, as well as wider age ranges, are needed to investigate the developmental trajectories of white matter microstructure.

Data and code availability statement

The datasets generated and/or analyzed during the current study are not publicly available due to legal and ethical regulations, but may be made available upon request to the Director of the Generation R Study, Vincent Jaddoe (v.jaddoe@erasmusmc.nl), in accordance with the local, national, and European Union regulations. The code used for the analyses of this study is available upon request to the first author, Mónica López-Vicente (m.lopez-vicente@erasmusmc.nl). The code used to generate the figures showing the age and sex associations with the DTI metrics of the tracts can be found in https://github.com/muet0005/YNIMG_117643.

Funding

This project has received funding from the European Union's Horizon 2020 research and innovation programme under the Marie Skłodowska-Curie grant agreement No 707404 (M.L.V.). The opinions expressed in this document reflect only the author's view. The European Commission is not responsible for any use that may be made of the information it contains. Additional support for this study was through the Netherlands Organization for Health Research and Development (ZonMw) TOP project number 91211021 (T.W.), the Simons Foundation Autism Research Initiative (SFARI – 307280, T.W.), Sophia Research Foundation (S18-20, R.L.M.), and the Erasmus University Fellowship (R.L.M.). The funding agencies were not involved in the study design; the collection,

analysis and interpretation of data; in the writing of the report; nor in the decision to submit the article for publication.

Authorship contribution statement

Mónica López-Vicente: Conceptualization, Methodology, Formal analysis, Writing - Original Draft, Visualization, Funding acquisition. **Sander Lamballais:** Methodology, Writing - Review & Editing. **Suzanne Louwen:** Data Curation, Writing - Review & Editing. **Manon Hillegers:** Resources, Writing - Review & Editing, Supervision. **Henning Tiemeier:** Writing - Review & Editing, Supervision, Project administration. **Ryan L. Muetzel:** Conceptualization, Methodology, Software, Formal analysis, Writing - Original Draft, Project administration, Funding acquisition. **Tonya White:** Conceptualization, Writing - Review & Editing, Project administration, Funding acquisition.

Declaration of Competing Interest

None.

Acknowledgements

The Generation R Study is conducted by the Erasmus Medical Center in close collaboration with Faculty of Social Sciences of the Erasmus University Rotterdam, the Municipal Health Service Rotterdam area, Rotterdam, and the Stichting Trombosedienst & Artsenlaboratorium Rijnmond (STAR-MDC), Rotterdam. We gratefully acknowledge the contribution of children and parents, general practitioners, hospitals, midwives, and pharmacies in Rotterdam.

Supplementary materials

Supplementary material associated with this article can be found, in the online version, at doi:10.1016/j.neuroimage.2020.117643.

References

Andersen, KW, Siebner, HR., 2018. Mapping dexterity and handedness: recent insights and future challenges. Curr. Opin. Behav. Sci. 20, 123–129.
Barnea-Goraly, N, Menon, V, Eckert, M, et al., 2005. White matter development during childhood and adolescence: a cross-sectional diffusion tensor imaging study. Cereb. Cortex 15 (12), 1848–1854.
Bartzokis, G, Lu, PH, Tingus, K, et al., 2010. Lifespan trajectory of myelin integrity and maximum motor speed. Neurobiol. Aging. 31 (9), 1554–1562.
Basser, PJ, Mattiello, J, LeBihan, D., 1994. MR diffusion tensor spectroscopy and imaging. Biophys. J. 66 (1), 259–267.
Basser, PJ, Pierpaoli, C., 1996. Microstructural and physiological features of tissues elucidated by quantitative-diffusion-tensor MRI. J. Magn. Reson. B. 111 (3), 209–219.
Benjamini, Y, Hochberg, Y., 1995. Controlling the false discovery rate: a practical and powerful approach to multiple testing. J. R. Stat. Soc. 57 (1), 289–300.
Brouwer, RM, Mandl, RCW, Schnack, HG, et al., 2012. White matter development in early puberty: a longitudinal volumetric and diffusion tensor imaging twin study. PLoS One 7 (4), e32316.
Cascio, CJ, Gerig, G, Piven, J., 2007. Diffusion tensor imaging: Application to the study of the developing brain. J. Am. Acad. Child Adolesc. Psychiatry 46 (2), 213–223.
Chang, LC, Jones, DK, Pierpaoli, C., 2005. RESTORE: robust estimation of tensors by outlier rejection. Magn. Reson. Med. 53 (5), 1088–1095.
Chiang, M-C, Barysheva, M, Shattuck, DW, et al., 2009. Genetics of brain fiber architecture and intellectual performance. J. Neurosci. Off. J. Soc. Neurosci. 29 (7), 2212–2224.
Clayden, JD, Jentschke, S, Muñoz, M, et al., 2012. Normative development of white matter tracts: similarities and differences in relation to age, gender, and intelligence. Cereb. Cortex 22 (8), 1738–1747.
Cook, PA, Bai, Y, Nedjati-Gilani, S, et al., 2006. Camino: open-source diffusion-MRI reconstruction and processing. In: 14th Sci. Meet. Int. Soc. Magn. Reson. Med., p. 2759.
Crone, EA, Elzinga, BM., 2015. Changing brains: how longitudinal functional magnetic resonance imaging studies can inform us about cognitive and social-affective growth trajectories. Wiley Interdiscip. Rev. Cognit. Sci. 6 (1), 53–63.
de Groot, M, Ikram, MA, Akoudad, S, et al., 2015. Tract-specific white matter degeneration in aging: the Rotterdam Study. Alzheimers Dement. 11 (3), 321–330.
Eluvathingal, TJ, Hasan, KM, Kramer, L, et al., 2007. Quantitative diffusion tensor tractography of association and projection fibers in normally developing children and adolescents. Cereb. Cortex 17 (12), 2760–2768.
Giedd, JN, Blumenthal, J, Jeffries, NO, et al., 1999. Development of the human corpus callosum during childhood and adolescence: a longitudinal MRI study. Prog. Neuropsychopharmacol. Biol. Psychiatry 23 (4), 571–588.
Giedd, JN, Blumenthal, J, Jeffries, NO, et al., 1999. Brain development during childhood and adolescence: a longitudinal MRI study. Nat. Neurosci. 2 (10), 861–863.
Giorgio, A, Watkins, KE, Chadwick, M, et al., 2010. Longitudinal changes in grey and white matter during adolescence. NeuroImage 49 (1), 94–103.
Gogtay, N, Giedd, JN, Lusk, L, et al., 2004. Dynamic mapping of human cortical development during childhood through early adulthood. Proc. Natl. Acad. Sci. USA 101 (21), 8174–8179.
Gorgolewski, K, Burns, CD, Madison, C, et al., 2011. Nipype: a flexible, lightweight and extensible neuroimaging data processing framework in python. Front. Neuroinform. 5, 13.
Grohs, MN, Reynolds, JE, Dewey, D, et al., 2018. Corpus callosum microstructure is associated with motor function in preschool children. NeuroImage 183, 828–835.
Haselgrove, JC, Moore, JR., 1996. Correction for distortion of echo-planar images used to calculate the apparent diffusion coefficient. Magn. Reson. Med. 36 (6), 960–964.
Jaddoe, VWV, Mackenbach, JP, Moll, HA, et al., 2006. The Generation R Study: design and cohort profile. Eur. J. Epidemiol. 21 (6), 475–484.
Jenkinson, M, Beckmann, CF, Behrens, TE, et al., 2012. FSL. Neuroimage 62 (2), 782–790.
Jenkinson, M, Smith, S., 2001. A global optimisation method for robust affine registration of brain images. Med. Image Anal. 5 (2), 143–156.
Jones, DK, Cercignani, M., 2010. Twenty-five pitfalls in the analysis of diffusion MRI data. NMR Biomed. 23 (7), 803–820.
Kooijman, MN, Kruithof, CJ, van Duijn, CM, et al., 2016. The Generation R Study: design and cohort update 2017. Eur. J. Epidemiol. 31 (12), 1243–1264.
Krogsrud, SK, Fjell, AM, Tamnes, CK, et al., 2016. Changes in white matter microstructure in the developing brain-a longitudinal diffusion tensor imaging study of children from 4 to 11years of age. NeuroImage 124, 473–486 (Pt A).
Lebel, C, Beaulieu, C., 2011. Longitudinal development of human brain wiring continues from childhood into adulthood. J. Neurosci. Off. J. Soc. Neurosci. 31 (30), 10937–10947.
Lebel, C, Caverhill-Godkewitsch, S, Beaulieu, C., 2010. Age-related regional variations of the corpus callosum identified by diffusion tensor tractography. NeuroImage 52 (1), 20–31.
Lebel, C, Treit, S, Beaulieu, C., 2019. A review of diffusion MRI of typical white matter development from early childhood to young adulthood. NMR Biomed. 32 (4), e3778.
Lebel, C, Walker, L, Leemans, A, et al., 2008. Microstructural maturation of the human brain from childhood to adulthood. Neuroimage 40 (3), 1044–1055.
Leemans, A, Jones, DK., 2009. The B-matrix must be rotated when correcting for subject motion in DTI data. Magn. Reson. Med. 61 (6), 1336–1349.
LeWinn, KZ, Sheridan, MA, Keyes, KM, et al., 2017. Sample composition alters associations between age and brain structure. Nat. Commun. 8 (1), 874.
Luciana, M., 2013. Adolescent brain development in normality and psychopathology. Dev. Psychopathol. 25, 1325–1345 (4 0 2).
McKay, NS, Iwabuchi, SJ, Häberling, IS, et al., 2017. Atypical white matter microstructure in left-handed individuals. Laterality 22 (3), 257–267.
Muetzel, RL, Collins, PF, Mueller, BA, et al., 2008. The development of corpus callosum microstructure and associations with bimanual task performance in healthy adolescents. Neuroimage 39 (4), 1918–1925.
Muetzel, RL, Mous, SE, van der Ende, J, et al., 2015. White matter integrity and cognitive performance in school-age children: a population-based neuroimaging study. Neuroimage 119, 119–128.
Muetzel RL, Mulder RH, Lamballais S, et al. Frequent bullying involvement and brain morphology in children. Front. Psychiatry. 2019;10:696.
Muftuler, LT, Davis, EP, Buss, C, et al., 2012. Development of white matter pathways in typically developing preadolescent children. Brain Res. 1466, 33–43.
Nagy, Z, Westerberg, H, Klingberg, T., 2004. Maturation of white matter is associated with the development of cognitive functions during childhood. J. Cognit. Neurosci. 16 (7), 1227–1233.
Nucifora, PGP, Wu, X, Melhem, ER, et al., 2012. Automated diffusion tensor tractography: implementation and comparison to user-driven tractography. Acad. Radiol. 19 (5), 622–629.
Oldfield, RC., 1971. The assessment and analysis of handedness: the Edinburgh inventory. Neuropsychologia 9 (1), 97–113.
Pasternak, O, Kelly, S, Sydnor, VJ, et al., 2018. Advances in microstructural diffusion neuroimaging for psychiatric disorders. NeuroImage 182, 259–282.
Paus, T., 2010. Population neuroscience: why and how. Hum. Brain Mapp. 31 (6), 891–903.
Paus, T., 2010. Growth of white matter in the adolescent brain: myelin or axon? Brain Cognit. 72 (1), 26–35.
Peirce, JW., 2008. Generating stimuli for neuroscience using psychoPy. Front. Neuroinform. 2, 10.
Perrin, JS, Hervé, P-Y, Leonard, G, et al., 2008. Growth of white matter in the adolescent brain: role of testosterone and androgen receptor. J. Neurosci. Off. J. Soc. Neurosci. 28 (38), 9519–9524.
Peters, BD, Ikuta, T, DeRosse, P, et al., 2014. Age-related differences in white matter tract microstructure are associated with cognitive performance from childhood to adulthood. Biol. Psychiatry 75 (3), 248–256.
Qiu, D, Tan, L-H, Zhou, K, et al., 2008. Diffusion tensor imaging of normal white matter maturation from late childhood to young adulthood: voxel-wise evaluation of mean diffusivity, fractional anisotropy, radial and axial diffusivities, and correlation with reading development. NeuroImage 41 (2), 223–232.
R Core Team, 2014. R: a Language and Environment for Statistical Computing.
Rosseel, Y., 2012. lavaan: an R package for structural equation modeling. J. Stat. Softw. 48 (2), 1–36.
Rubin, DB., 2004. Multiple Imputation for Nonresponse in Surveys. John Wiley & Sons, p. 326.

Schmahmann, J., 2009. Fiber Pathways of the Brain. Oxford University Press, USA, p. 674 p.
Schmahmann, JD, Pandya, DN, Wang, R, et al., 2007. Association fibre pathways of the brain: parallel observations from diffusion spectrum imaging and autoradiography. Brain J. Neurol. 130, 630–653 Pt 3.
Schmithorst, VJ, Wilke, M, Dardzinski, BJ, et al., 2005. Cognitive functions correlate with white matter architecture in a normal pediatric population: a diffusion tensor MRI study. Hum. Brain Mapp. 26 (2), 139–147.
Schmithorst, VJ, Yuan, W., 2010. White matter development during adolescence as shown by diffusion MRI. Brain Cognit. 72 (1), 16–25.
Simmonds, DJ, Hallquist, MN, Asato, M, et al., 2014. Developmental stages and sex differences of white matter and behavioral development through adolescence: a longitudinal diffusion tensor imaging (DTI) study. Neuroimage 92, 356–368.
Smith, SM., 2002. Fast robust automated brain extraction. Hum. Brain Mapp. 17 (3), 143–155.
Statistics Netherlands, 2004. Allochtonen in Nederland 2004. Voorburg/Heerlen (https://www.cbs.nl/nl-nl/publicatie/2004/50/allochtonen-in-nederland-2004). (Accessed October 1, 2020).
Tamnes, CK, Roalf, DR, Goddings, A-L, et al., 2018. Diffusion MRI of white matter microstructure development in childhood and adolescence: methods, challenges and progress. Dev. Cognit. Neurosci. 33, 161–175.
Thompson, PM, Giedd, JN, Woods, RP, et al., 2000. Growth patterns in the developing brain detected by using continuum mechanical tensor maps. Nature 404 (6774), 190–193.
van Buuren, S, Groothuis-Oudshoorn, CGM, 2011. mice: Multivariate Imputation by Chained Equations in R. J. Stat. Softw. 45 (3). [electronic article] https://research.utwente.nl/en/publications/mice-multivariate-imputation-by-chained-equations-in-r . (Accessed November 23, 2019).
Van Wittenberghe, IC, Peterson, DC., 2020. Neuroanatomy, Corticospinal Tract Lesion. StatPearls InTreasure Island (FL): StatPearls Publishing(Accessed May 18, 2020)(http://www.ncbi.nlm.nih.gov/books/NBK542201/). (Accessed May 18, 2020).
Weisskopf, MG, Sparrow, D, Hu, H, et al., 2015. Biased exposure-health effect estimates from selection in cohort studies: are environmental studies at particular risk? Environ. Health Perspect. 123 (11), 1113–1122.
Westerhausen, R, Kreuder, F, Sequeira, SDS, et al., 2004. Effects of handedness and gender on macro- and microstructure of the corpus callosum and its subregions: a combined high-resolution and diffusion-tensor MRI study. Cognit. Brain Res. 21 (3), 418–426.
White, T, El Marroun, H, Nijs, I, et al., 2013. Pediatric population-based neuroimaging and the Generation R Study: the intersection of developmental neuroscience and epidemiology. Eur. J. Epidemiol. 28 (1), 99–111.
White, T, Muetzel, RL, El Marroun, H, et al., 2018. Paediatric population neuroimaging and the Generation R Study: the second wave. Eur. J. Epidemiol. 33 (1), 99–125.
Yakovlev, P, Lecours, AR., 1967. The myelogenetic cycles of regional maturation of the brain. In: Regional Development of the Brain in early Life. Blackwell Scientific Publications, Oxford, pp. 3–70.